PAPER REF: 3910

A MICROSCOPIC FAILURE ANALYSIS OF MEDIUM TRUCK BRAKE DISCS

Arie Bussiba[1(*)], Rami Carmi[1], Igal Alon[1]

[1]Nuclear Research Center Negev, P. O. Box 9001, Beer Sheva, Israel

[(*)] *Email:* busarie@bezeqint.net

ABSTRACT

Routine checkup of security vehicle, together with drivers` complaints of abnormal vibrations during the braking process, indicates a severe damage of brake discs in terms of radial macro-crack and heavily micro-cracks on the friction surfaces. This failure occurs after a short period of service (less than 15000 km) and significant damage was also noticed in brake disc that was removed after 6000 km. Although the characteristics driving in such vehicle are accompanied by high speed with high g-deceleration frequently, it's still an abnormal failure. The inquiry process of the concerned ones indicates that some modifications have been made which considerably increases the total mass of the vehicle. This change significantly affects the forces acting on the brake disc and accordingly on the temperature evolution during the braking process. This change was not involved with any adjustment in the braking system. Comprehensive microscopic examination (metallographic, fractographic together with chemical analysis and mechanical testing) of the gray iron brake discs enables to point out some additional sources which lead to this precursory failure. Possible solutions were suggested in order to prevent such damage which can be hazardous to proper functionality of this safety component. Firstly, to replace the brake disc more often based on the fatigue crack initiation study. Secondly, to consider using new structural material such as AISI 4330 with a higher endurance fatigue limit and with great resistance to thermal fatigue crack initiation.

Keywords: brake disc (rotor), gray iron, micro/macro cracks, thermal fatigue.

INTRODUCTION

The brake discs are subjected to various macro and microscopic damages especially during severe operating , typical to emergency and security vehicles. At these heavy breaking loads and high g-declarations, the damage appeared in different types such as heat cracks and crazing (Bagnoli, 2009, Mackin, 2002), wear, grooves, hard spots (Panier, 2004), blue coloring, microstructure changes (Sakamoto, 2005) and distortions (Murphy, 2009). These types of damages resulted from the braking process which convert the vehicle's kinetic energy into thermal energy before releasing it into the surroundings. Extremely hot spots at temperatures higher than the AC_1 transformation temperature (approximately 750°C) are developed in a very shallow layer under the friction surface of the disc (Yamabe 2003). Due to thermal gradients, the friction surface of the rotor undergoes compressive stresses accompanied by plastic deformation (Bagnoli, 2009) and by cooling, residual tensile stress is generated in these spots. Heat cracks are being initiated in the friction surface due to thermal stress cycling. Beside the above mentioned local temperature gradient, additional temperature gradient develops between the friction surface average temperature (some 500°C) and the rotor inside temperature. This surface/inside temperature gradient is a macroscopic or average temperature gradient in contrast to local of the former one. Repeated thermal stress caused by this average temperature gradient controls the propagation stage of the heat cracks. Thus, the heat cracks initiate at a very early stage of brake application due to the high thermal stresses. The service life of a rotor, is considered to be governed by the propagation life of heat cracks after they have initiated (Yamabe 2003).

During the braking process the mentioned severe damages may cause brake fade, brake fluid vaporizes, bearing failure and thermally–excited vibration, phenomena which affect the operability and performance of this safety component. The degradation in braking efficiency is highly dependent on the drivers` habits.

The current investigation deals with the failure of brake disc of medium truck security vehicle, which was noticed after a short time of service. It was reported that the vehicle undergoes some chassis modifications which increase its total weight by more than 30% without any adjustment in the braking system. The failure analysis scheme initiated with visual inspection of both friction surfaces, focused on the main cracks location and orientation, as for the micro-cracks density, crack opening, dimensions and distribution were characterized. Optical microscopy was used to reveal the microstructure of the gray iron material, with special attention to the preferred metallurgical sites in cracking initiation and propagation stages. The fracture surface of the main crack was exposed carefully by monotonic controlled loading. The fracture modes and the crack shape through thickness were classified by utilizing scanning electron microscopy. Finally, specimens with rectangular geometry were prepared from the damaged area and were fatigue loaded until the crack was formed by micro-cracks coalescence process. The fatigue "pre-cracked" specimens were then loaded up to fracture, and the simulated fracture was examined in comparison with the original one due to thermal fatigue.
Based on the experimental findings two recommendations have been suggested; one is related to maintenance and the other has a metallurgical/mechanical aspect attributed in replacing the structural material of the brake disc.

EXPERIMENTAL PROCEDURES

Two brake discs were examined; one (noted rotor 1) was removed after 15000 km of service which contain a through thickness macro-crack (Fig. 1a) while the second (noted rotor 2) was taken out after 6000 km of operating with no indication of macro damage (Fig. 1b). The visual inspection was carried out after soft polishing of the surface rim in order to get rid of dust and oxidation debris.

The macro damage was documented by means of Canon camera with a macro lens feature. The micro damage and the material microstructure were characterized using light microscopy with magnification up to X500. Attention was given to possible changes in the microstructure at different areas of the rim. Simultaneously, chemical analysis was done by wet and arc spark methods to determine the exact iron alloy.
Hardness measurements were performed in radial orientation from the inner to the outer region of the rim on the lock bolts side. For comparison, hardness was conducted at the rim on the vehicle side as well as in the hub.
In order to expose the fracture surface of the macro crack, the rim was cut so that the part included the crack was loaded at flexural mode using four point device. Fig. 2a depicts a general view of the experimental set-up, while Fig. 2b shows the crack direction with respect of the inner loading cylinders.

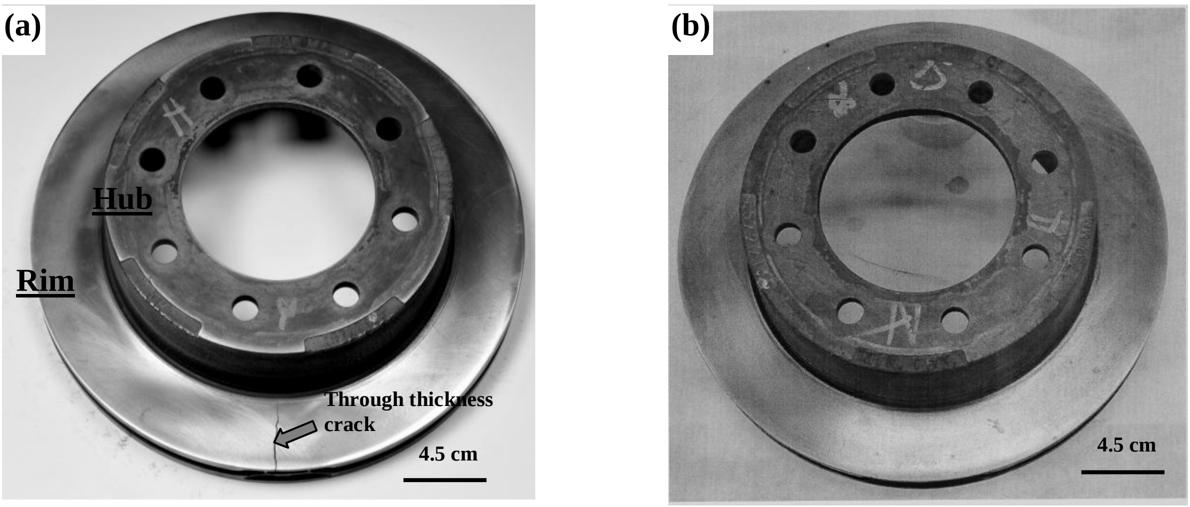

Fig. 1 The analyzed brake discs (lock bolts side); (a) cracked rotor 1, removed after service of 15000 km, (b) un-cracked rotor 2 removed after 6000 km of service.

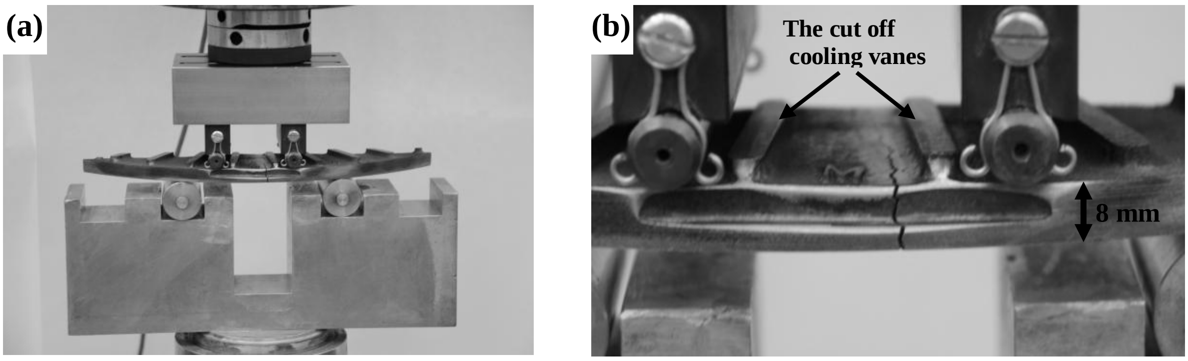

Fig. 2 The cracked segment loaded in four point apparatus device; (a) general view, (b) the location of the crack with relation to the inner loading cylinders.

The fracture modes associated with the revealed surface were classified by scanning electron microscopy focused on crack initiation sites, as well as on the features morphology of the stable crack growth region.

To estimate the damage degree in an area far away from the main crack, uniform rectangular specimens with dimensions of 10X8X55 mm were prepared from the rim in peripheral orientation. The specimens were fatigue loaded in computerized electro resonance machine in bending mode with sinusoidal wave form (Figs. 3a-b). The load ratio was selected to be 0.1 and the maximum bending stress was 170 MPa, half of the approximated quasi-static bending stress 340 MPa, estimated from the chemical composition and hardness of the virgin material (see later on). The applied bending stress was calculated from the analytical equation $\sigma=Mc/I$ (M=moment, c half of the specimen height and I moment of inertia). For comparison, undamaged specimens were loaded in the same fatigue conditions. Metallographic and fractographic studies were conducted on mechanical fatigued specimens with focused on the preferred cracking sites and fatigue fracture modes.

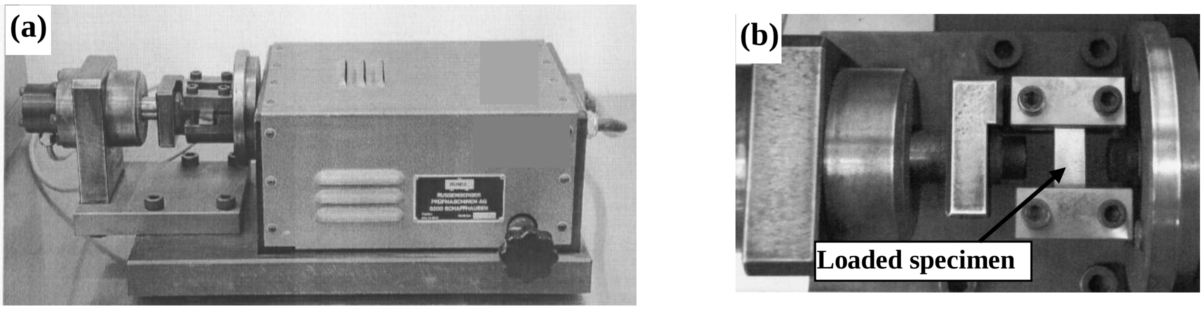

Fig. 3 Electro resonance system; (a) general view, (b) loaded cracked specimen.

EXPERIMENTAL RESULTS

Chemical analysis

Chemical analysis of both rotors revealed that the main present elements are, C, Si and Mn and microstructure consist of graphite flakes within pearlitic matrix with lamellar morphology (see later on); indicate that the structural material utilized for this automotive component is flake cast iron. A content of 2.95% C, 1.95% Si, and 0.8% Mn with some traces of 0.25% Cr, classified this iron alloy as a GG25 cast iron (Vonroll Casting) with the following mechanical properties; tensile strength of about 350 MPa, yield point of 228 MPa with elongation less than 0.5% and with bending strength of about 340 MPa. The hardness Brinell is in the range of 180 to 200 HB.

Macro and microscopic damages

The macroscopic damage in rotor 1 in terms of through thickness crack is shown in Figs. 4a-d in different views indicating three major points; (1) the crack propagated from the exterior part of the rim to the interior one and was arrested at the hub / rim interface (Fig. 4a). This argument is based on the fact that high crack opening is involved at the exterior part (Fig. 4c) and decrease as the crack extended toward the interface hub/rim. (2) The crack propagated at the area where the material was removed by machining for balance consideration (Fig. 4b) (noted by dashed arrows). (3) The crack was initiated near the radius of the cooling vanes (Fig. 4c) and growth along the edge vane (Fig. 4d). The last two preferred cracking sites point out on the high sensitivity of this material to geometrical irregularities which act as local stress intensification. This mechanical response is related to the low ductility (less than 0.5% of elongation) of this brittle material.

The major crack in rotor 1 was followed by heavily micro-cracking with some radial cracks which extend the trace of pad width as illustrated by two circumferential dashed lines (Fig. 5a). As shown the macro-mechanism of the main crack is the coalescence process of the micro-cracks as noted at the friction surface for some potential sites for macro-crack initiation. The extents of these cracks are in the range of 1-5 mm and the depth varied between 50μm up to 0.3 mm (Fig. 6a) . As demonstrated, the crack origin is a pit, resulted from the preferred oxidation process at graphite flakes (marked by a dashed line). After reaching a critical pit length (around 100μm), crack initiation followed by the crack propagation stage which is being controlled mainly by mechanical process. The crack extended through the graphite flake (see arrows in Fig. 6b) and later on at the interface graphite flaks/pearlitic phase. These findings indicate on the low resistance to chemical and mechanical processes of the brittle graphite phase. The preliminary damage appears in terms of the micro-cracking network as shown in Fig. 5b for the rotor 2 which was removed after only 6000 km. This form of damage is related to the presence of graphite flakes distributed randomly in the pearlitic matrix, the typical microstructure of this material as will be shown later on.

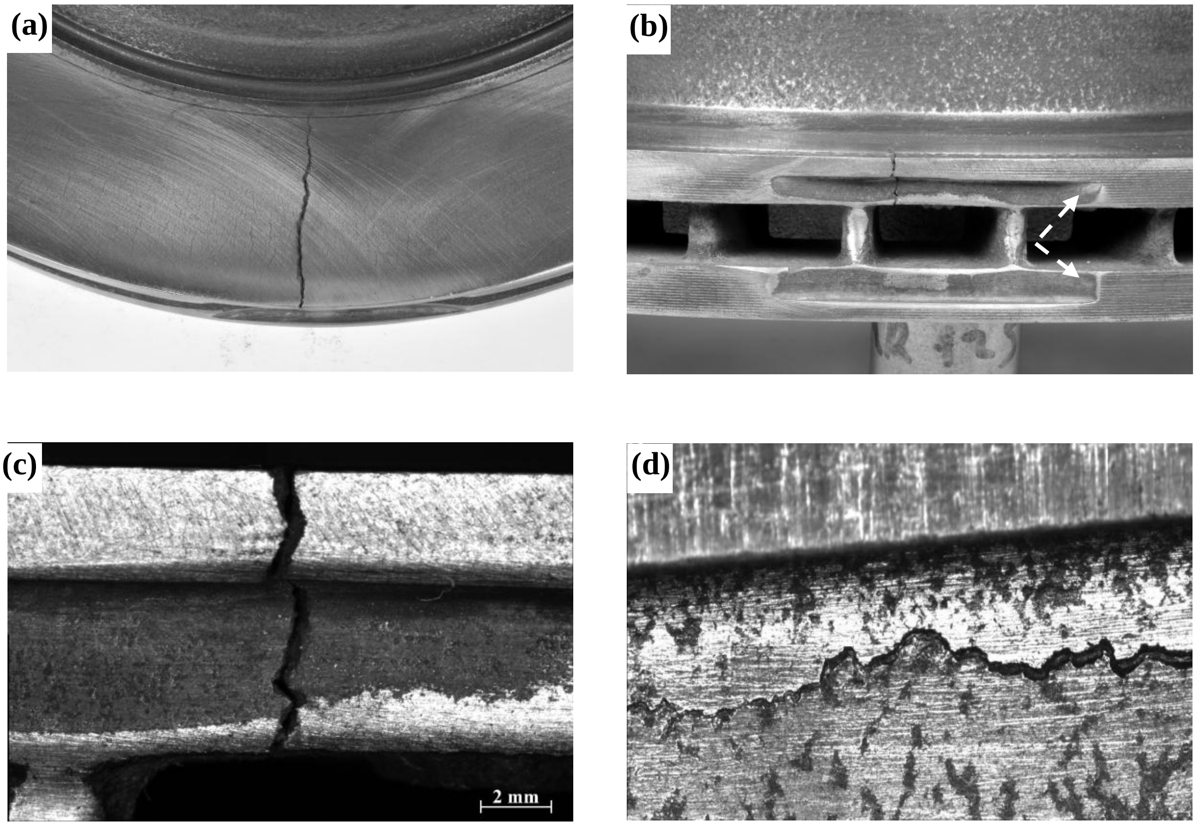

Fig. 4 Different views of the macroscopic crack ; (a) rim top view, (b-c) side view depicted the crack preferred location, (d) the crack path in the vicinity of the wall van (view from the interior part of the rim).

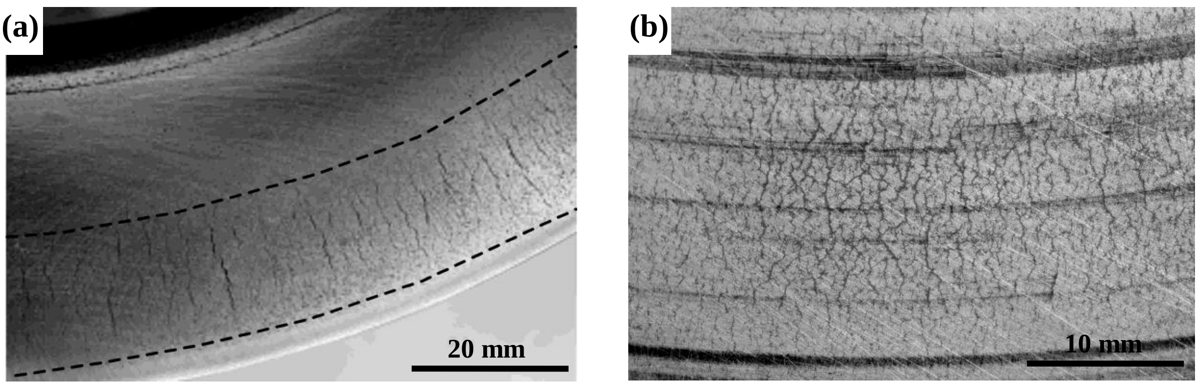

Fig. 5 Different types of microscopic damages; (a) radially orientated micro-cracks in rotor 1, (b) micro-cracks network in rotor 2.

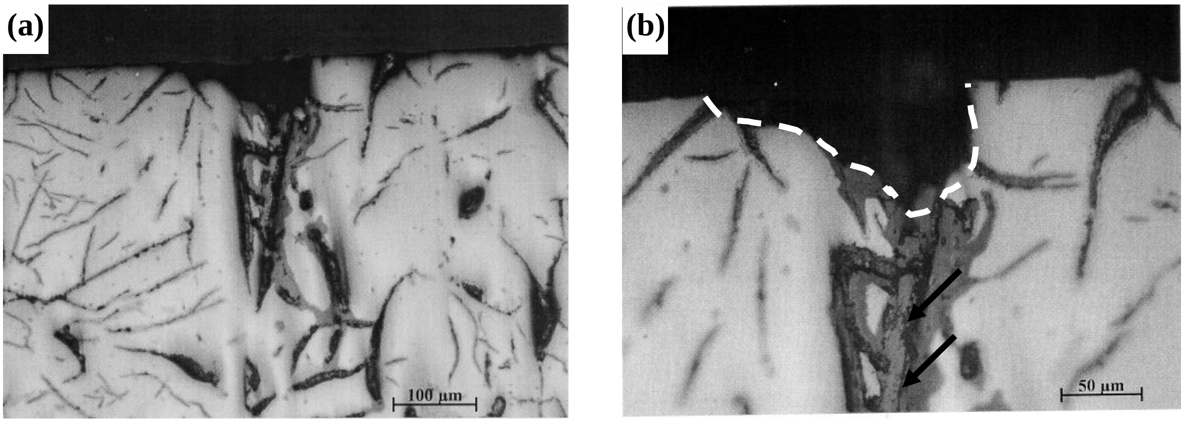

Fig. 6 The depth and the preferred sites of the micro-cracks initiation; (a) pit as a source for crack initiation, (b) crack propagates through graphite flake.

Microstructure and hardness changes

Figs. 7a and 7b illustrate the microstructure of the cast iron from the hub part, far away from the rim, which was exposed to high temperature due to braking cycle. As shown, the polished condition reveals random flake graphite in a uniform distribution which characterized A type graphite distribution in gray cast iron. Etching procedure exposed the graphite flakes within the pearlitic matrix accompanied by lamellar morphology; no evidence of ferritic or retained austenitic phases were detected.

Tracking the microstructure within the friction zone of the rim indicate some phases modification. The microstructure at the rim interior (near the hub) was almost the same as the one shown in Fig. 7b. In the vicinity of the pad, traces of the ferrite phase were detected (see arrows in Fig. 8b), which grows from the graphite flakes interface during the cooling stage. In the middle and at the exterior of the rim, the content of the ferritic phase increases dramatically as shown in Fig. 8d. The flake graphite content and morphology were not altered due to the heating-cooling cycles. The presence of ferrite phase causes to a decrease in the tensile strength as also manifested by low values of hardness with average of 82RB (153 HB) as compared to an average of 92HB (190 HB) in the orginal microstructure. Following the ASM specialty handbook, this change in the hardness is corresponding to a decrease in the yield strength as well as the fatigue endurance limit (Cast iron ASM, 1996).

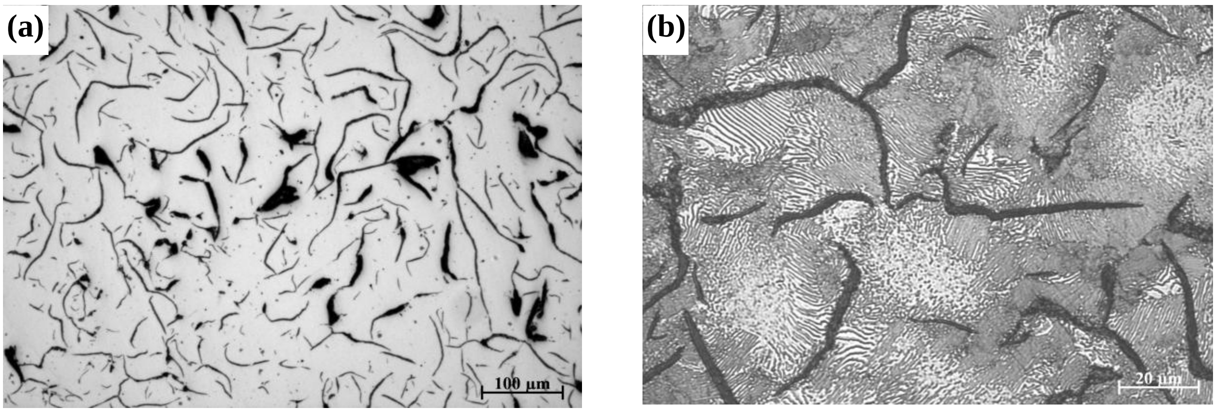

Fig. 7 Microstructure of the cast iron characterizes a 'virgin' material; (a) as polished illustrates the A type graphite with a flake-like morphology, (b) etched sample showing graphite flakes dispersed in a pearlitic structure.

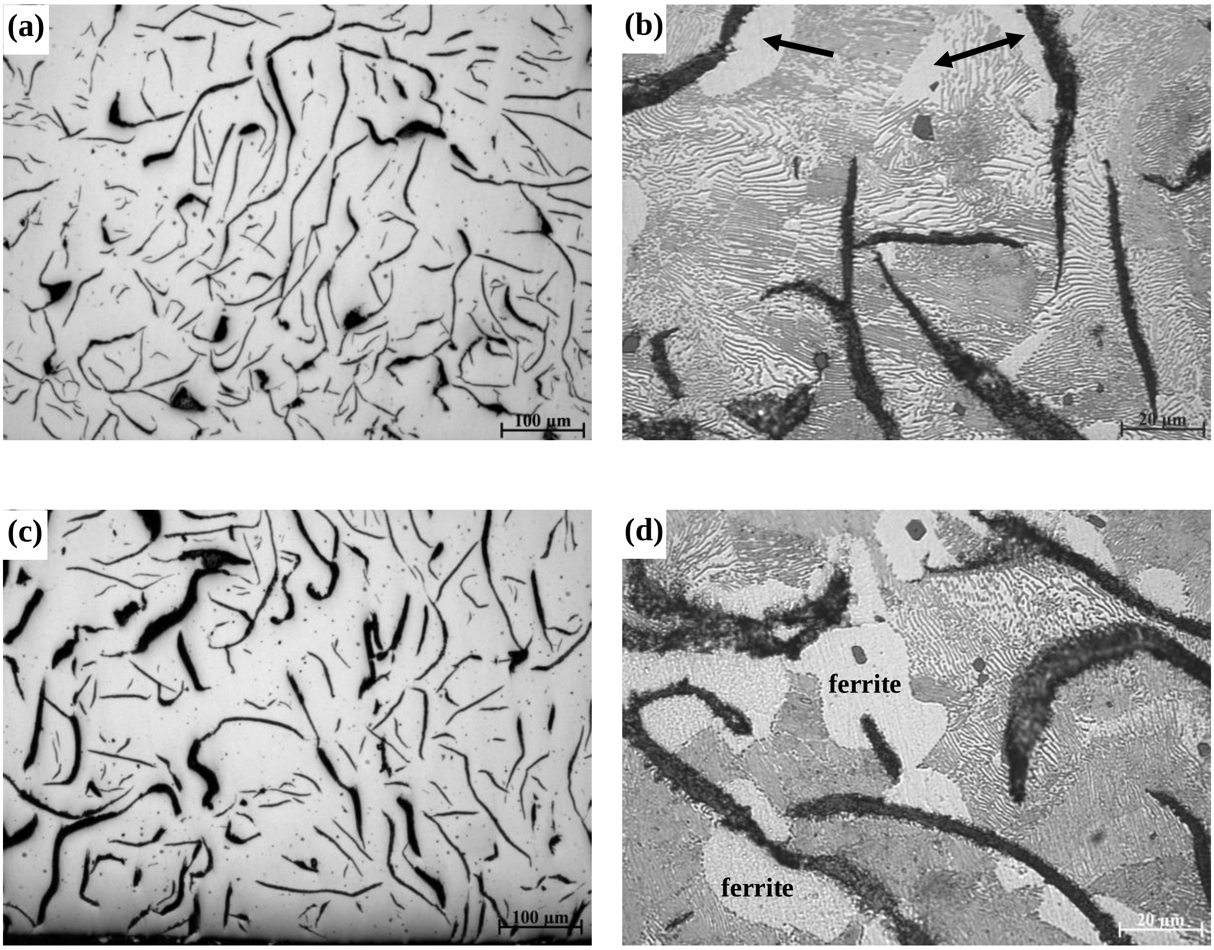

Fig. 8 Transition of the microstructure within the friction surface zone; (a-b) as polished and etched near the pad with some traces of ferittic phase, (c-d) as polished and etched at the exterior part of the pad with dominate content of ferittic phase.

Macro and microscopic fracture modes of the thermal fatigue crack

Figs. 9a-b show the macroscopic fracture mode of the main crack which was opened after controlled loading. As shown, most of the fracture surface is covered by oxides (Fig. 9a) with only isolated areas consist of fresh fracture features (Fig. 9b). The mechanical fracture is depicted in the upper right part of Fig.9a with coarse grain morphology.

Figs. 10a-d demonstrate the microscopic fracture modes of the crack growth. The pit incubation and growth stage form by the coalescence process of a series of micro holes as illustrated by a dashed line at the bottom of Fig. 10a. This stage was also shown by the metallographic study (see Fig. 6b). The transition to crack initiation stage is well emphasized by flat fracture with some areas characterized by low energy fracture surface. This smooth surface may be a result of oxidation combined with the fact that the crack propagates through and along the interface of the graphite flake. Some indication of thermal fatigue feature is depicted in Fig. 10b (see arrows) in the form of striations- like (similar to mechanical fatigue). Fig. 10c shows the mechanical fracture of the pearlite phase with the lamellar morphology. The brittleness of the graphite flake like cleavage mode surrounded by the pearlite phase is given in Fig. 10d.

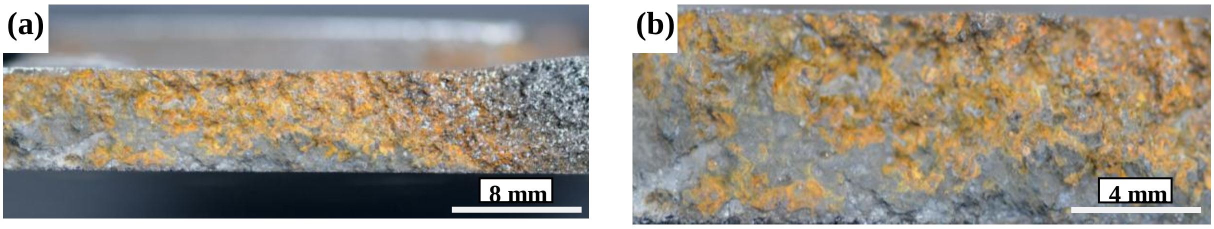

Fig. 9 Macroscopic fractures of thermal fatigue crack growth and mechanical crack

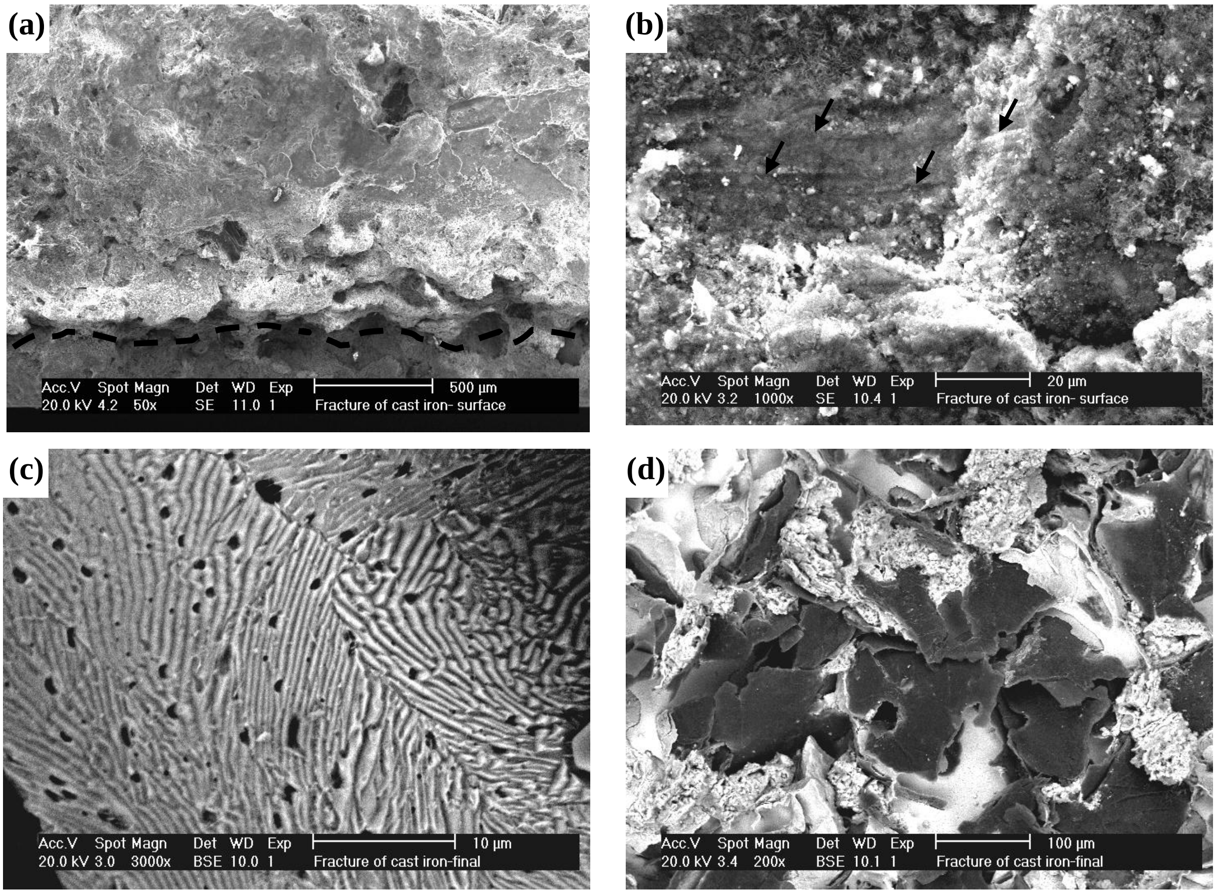

Fig. 10 Fracture modes of the thermal fatigue crack growth ; (a) pit morphology and transition to crack growth, (b) striations like , (c) pearlite fracture, (d) graphite flake fracture.

Macro and microscopic findings of the mechanical fatigue crack

The specimen taken from the damaged rim and was loaded in the resonance machine exhibits crack after 5.10^5 cycles as shown in Figs. 11a-d. The crack path with zigzag, branched and secondary cracking morphologies are shown in Fig. 11a. This type of crack extension is attributed to the preferred crack growth at the graphite flake interface as illustrated in Fig. 11b. In addition it seems that the crack propagates at the ferrite/graphite flake interface (see Fig. 8d). As mentioned the ferrite phase is present due to the heat/cooling cycle of the disk brake. The crack bridging mechanism is shown in Fig. 11d tracking after the adjacent preferred graphite flake.

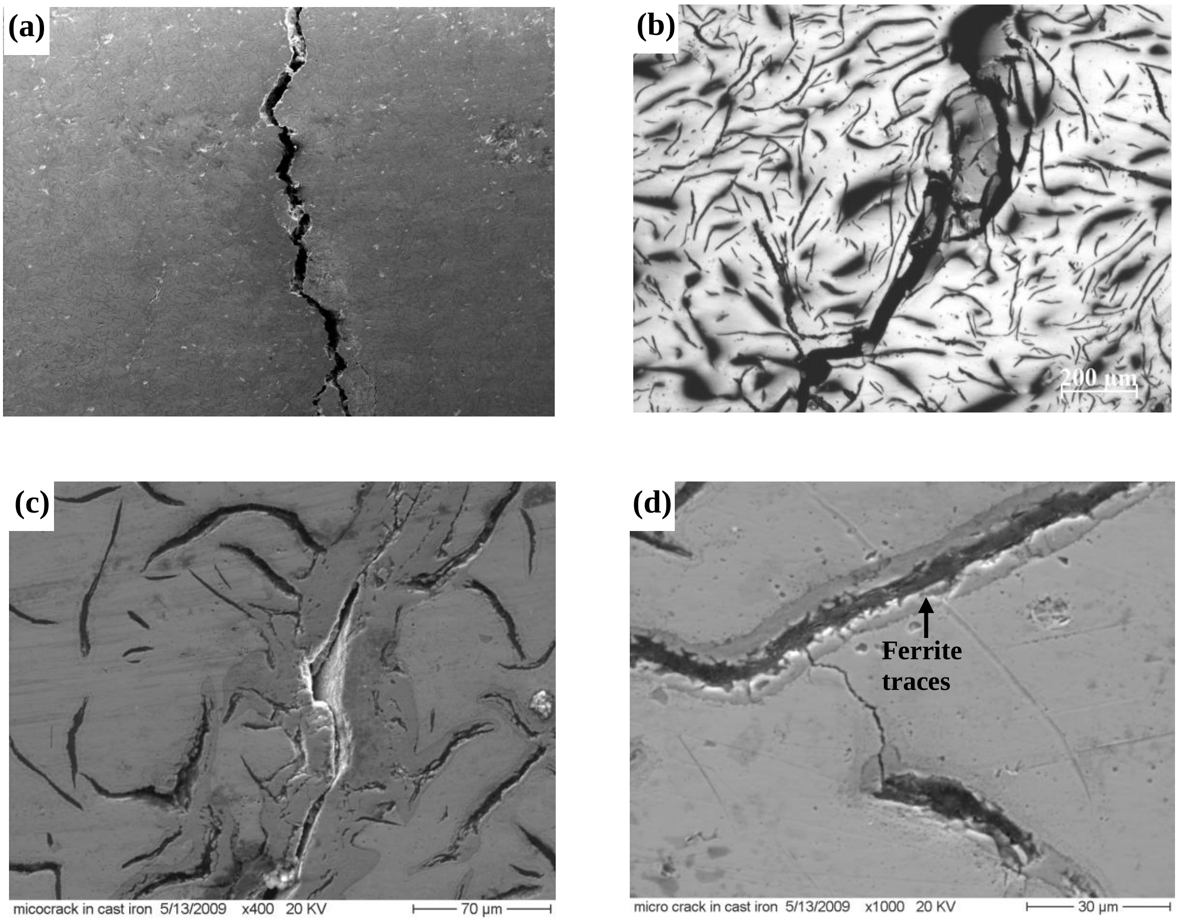

Fig. 11 The crack path morphology in the fatigue loaded specimen ; (a) macro-crack, (b) the crack following the graphite flake interface, (c) preferred crack growth at ferrite/graphite interface, (d) crack bridging mechanism.

Finally, the next Figs. depicted the fatigue fracture modes which are different from the ones obtained by thermal fatigue combined with oxidation of the fracture surface. Fig. 12a shows cleavage like fracture arises from the brittleness of the graphite flake which emphasized in Fig. 12b. In addition, as in the case of the thermal fatigue, the crack was initiated through or at the interface of the graphite flake. Fig. 12c shows fine features on the cleavage facet with hexagonal shape which may arise from the base plane of the HCP structure of the graphite. The lamellar morphology of the pearlitic phase is well reflected on the fracture surface (Fig. 12d) as already shown in Fig. 10c.

The reference specimen which was loaded in the same fatigue conditions exhibits more than $5x10^6$ cycles with no indication of macro or micro crack initiation. This finding points out qualitatively on the decreasing of the fatigue endurance limit, namely degradation in the fatigue resistance potential of the damaged friction surfaces.

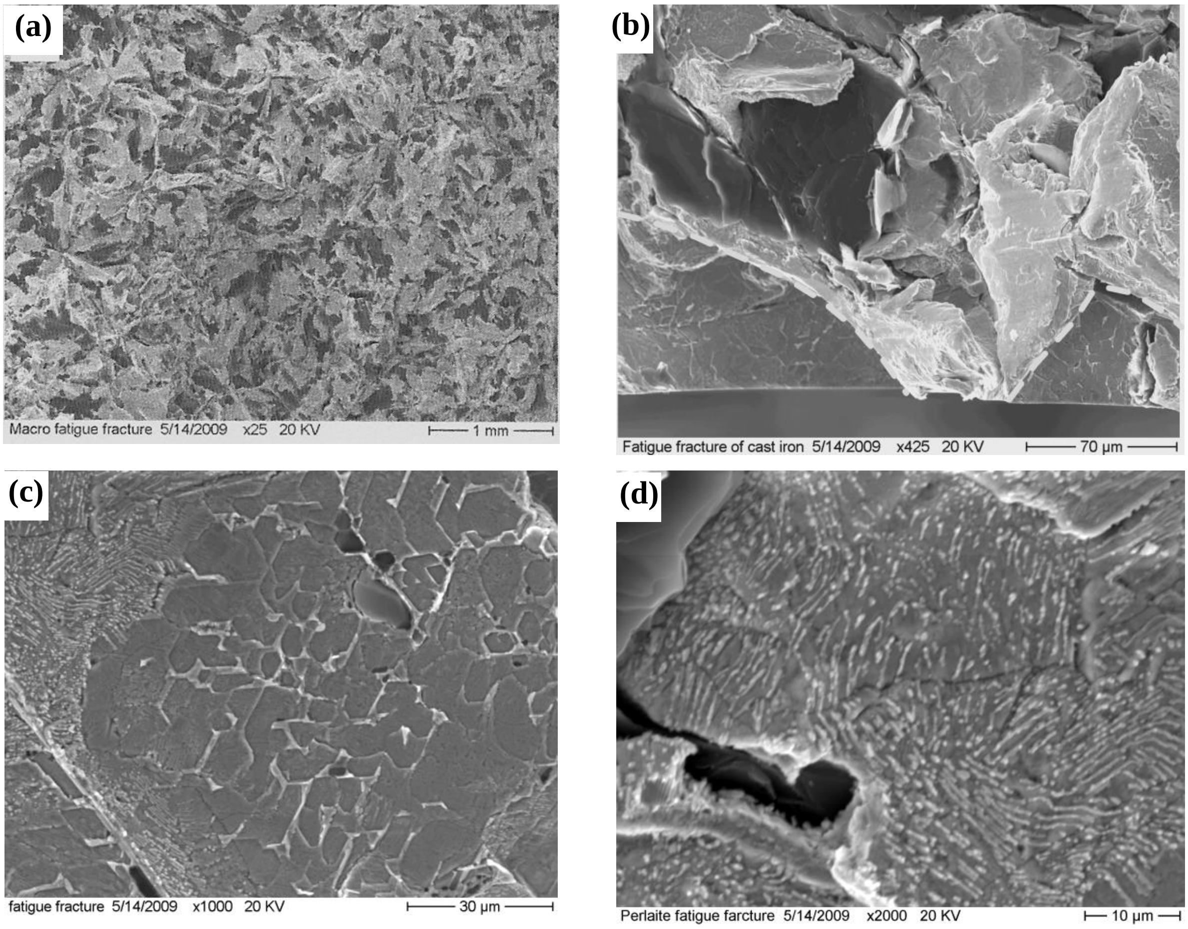

Fig. 12 Fatigue fracture modes obtained by mechanical cyclic loading ; (a) general view with cleavage like fracture, (b) fatigue crack initiation through graphite flake, (c) hexagonal traces on cleavage like of graphite flake, (d) lamellar fracture of the pearlitic phase.

DISCUSSION

The experimental findings point out that the early damage was initiated by mainly control chemical process at preferred sites of the graphite flakes. The damage at this stage was manifested by a series of pits which merged to a critical micro-crack which then propagate by thermal stresses. The propagation stage was characterized by micro-cracking coalescence mechanism to form a macro-crack. Although the fracture surface was covered by oxidation debris, isolated areas show some thermal fatigue features with striations like.

The fatigue tests show that the crack was initiated at the interface ferrite/graphite indication of low resistance to fatigue crack initiation. The mechanical fatigue testing exhibits different fracture modes compare to thermal fatigue, due to the difference in the strain amplitude (elastic as compared to a plastic one). However, this test procedure using a resonance machine with frequency decreasing criterion can be used to determine the damage degree after a specific service time. The data can be applied to decide on the replacing service time of the rotor rather than the recommended one.

The occurrence of crack development on the friction surface of a brake disc due to thermal cracking is not is a rare phenomenon when using this component far away from its service life recommended by the manufacturer or in extreme conditions of braking such as in an emergency or security vehicles. The current failure is categorized in the last case, however when dominant damage is initiated in a short interval of service (less than 15000 km), some clarifications are required from material, mechanical and driving habit aspects.

The chemical analysis, microstructure morphology of the present phases and the hardness values indicate on flake cast iron, material which is being used in the automotive industry for braking applications. The typical mechanical properties are in the range of 350-400 MPa in ultimate strength and 215-250 MPa in yield strength. Thus, from structural material consideration the designer made an appropriate and accepted selection of this safety component. As mentioned previously, the vehicle has been modified from security considerations resulted in an increase of more than 30% in its total mass. This change was not accompanied by any adjustment in the braking system. Obviously, such significant modification, influence on the force values, acting on the brake rotors and accordingly on the temperature arising during braking. The microstructure and hardness changes which have been noticed in the metallographic study (see Figs. 8b and 8d), indeed indicate on high temperature exposure during service of the rotor.

Based on Mackin, 2002 study on brake rotor similar to one investigated in the current study some comprehensions can be derived to our failure case. In general, his work intended to predict the fatigue lifetime of specific rotor in case of high g-braking, typical conditions for heavy duty vehicles such as in case of emergency or security medium trucks. Following mechanical and thermal analysis, heat flux equation related to braking forces was developed to determine the temperature profile in the brake and then estimate the arising stresses using a simplified shrink fit analysis. The calculated residual tensile hoop stresses exceed the yield strength which indicated that large tensile strains arise due to high g-braking. Using Manson-Coffine law, the number of fatigue cycles to failure was then predicted and was found with a good agreement with experiments (around 300 cycles). This prediction takes into account the mass vehicle and by increasing this parameter (as in our case) the tensile plastic strain will be altered to higher values due to exceptional temperatures. As known, in the low cycle fatigue regime, great dependence exists between the cycles to failure and the strain amplitude. Subsequently, the number of cycles to failure will reduce respectively. So, the precursory failure as occurred and illustrated in the current study in terms of through thickness crack is not unexpected. The relative contribution to this preliminary failure by reckless driving, characterized by heavy braking loads and high g-declarations are minor, due to the fact that the vehicle was designed to carry such extreme conditions.

Although the geometrical factors (radius of the cooling vans and areas where material was removed by machining for balance consideration) which act as local stress raisers, are factors from second order, but still may affect on the crack initiation time. In order to reduce the first element effect, it's necessary to increase the cooling vans radius, or alternatively to re-design the geometry profile of the cooling vans. For the second element, more caution is needed to be given during the manufacturing process such that no machining is required (Murphy, 2009).

In conclusion, in order to prevent or at least to reduce such failure, it has been suggested to replace the discs more often (the exact service time will be based on the fatigue crack initiation study) than recommended by the manufacturer due to the unique circumstances. Alternatively, to replace the conventional gray iron with flake graphite form to gray cast iron with graphite particles in the compact vermicular form (Goo and Lim, 2012) or by Ni addition and Ce inoculation to refine the graphite flakes (Yamabe et. al 2003) . The latter material has longer crack initiation lifetime than the conventional material. In addition, to use higher strength steel with stronger resistance for thermal fatigue loading. This trend is being done already in the Shinkansen train by using forged 1045 steel disc and lately also AISI modified 4330 (Sakamoto, 2005).

ACKNOWLEDGMENTS

The authors wish to express their gratitude to Mr. M. Cohen, Mr. S. Levy and G. Agronov from NRCN, for their experimental assistance.

REFERENCES

Bagnoli F, Dolce F, Bernabei M. Thermal fatigue cracks of fire vehicles gray iron brake discs. Engineering Failure Analysis 2009, 16, p. 152-163.

Cast iron. ASM specially handbook. 1996, p. 395-408.

Goo BC, Lim CH. Thermal fatigue of cast iron brake disk materials. Journal of Mechanical Science and Technology 2012, 26(6), p. 1719-1724.

Mackin JT, Noe SC, Ball KJ et al. Thermal cracking in disc brakes. Engineering Failure Analysis 2002, 9, p. 63-76.

Murphy C. The final word on brake Judder and “warped” discs. Powerbrake, www.powerbrake.co.za 2009, p. 1-8.

Panier S, Dufrénoy P, Weichert D. An experimental investigation of hot spots in railway disc brakes. Wear 2004, 256, p. 764–773.

Sakamoto H, Hirakawa K. Fracture analysis and material improvement of brake discs. JSME International Journal 2005, 48 (4), p. 458-464.

Yamabe J, Takagi M, Matsui T. Development of disc brake rotors for Heavy- and medium -duty trucks with high thermal Fatigue Strength. Technical Review 2003 No. 15, p 42-51.

W.W.W. vonroll-casting.ch